MICROBUNCHING INSTABILITY EFFECT STUDIES AND LASER HEATER OPTIMIZATION FOR THE SPARX FEL ACCELERATOR

C. Vaccarezza, E. Chiadroni, M. Ferrario, INFN-LNF, Frascati (Roma), Italy
G.Dattoli, L. Giannessi, M. Quattromini, C. Ronsivalle, ENEA C.R., Frascati (Roma), Italy
M.Venturini, LBNL, Berkeley, 94720 CA, USA
M. Migliorati, Rome University La Sapienza, Roma, Italy

Abstract

The effects of microbunching instability for the SPARX accelerator have been analyzed by means of numerical simulations. The laser heater counteracting action has been addressed in order to optimize the parameters of the compression system, either hybrid RF plus magnetic chicane or only magnetic, and possibly enhance the FEL performance.

INTRODUCTION

The FEL SPARX project will provide FEL radiation up to the region of X-rays and will accomplish this goal through successive steps [1]. The Electron beam characteristics suitable for the FEL operation are obtained after considerable beam manipulations, necessary to enhance the peak current. One of the problems consequent to an intensive beam handling is the emerging of undesired density modulations which may induce an instability yielding an additional energy spread, limiting the performances of the SASE process itself because it determines an increase of the process gain length, with a consequent increase of the saturation length.

The microbunching instability effect has been studied for the 1.5GeV accelerator configuration: two schemes have been analyzed for the bunch compression: the "hybrid" one , velocity bunching in the photoinjector plus a magnetic chicane (BC2) at E≈500 MeV, and the one based on a double magnetic compression at E≈300 MeV (BC1) and at E≈500 MeV (BC2). The insertion of a laser heater chicane is foreseen downstream the photoinjector and the two compression schemes have been analyzed by means of the laser heater effectiveness in dumping a superimposed beam density modulation. Numerical simulations have been carried on with the help of TSTEP and ELEGANT codes [3,4], the obtained results are presented and discussed in this paper.

THE ACCELERATOR

To reach the SASE saturation in the 1.5 GeV undulator (see Fig. 1) a peak current Ipk ≈1kA is required respectively, with a final rms slice spread <0.03 %. The main parameter list is reported in Table 1 where the nominal beam energy, peak current, rms normalized emittance ε_{nx}, rms energy spread σ_δ and correspondent radiation wavelength are indicated.

The SPARC photoinjector [5] provides the electron beam with energy ≈ 150MeV, the 1.5 GeV accelerator section ends with the Linac3 and the electron beam is delivered to the first undulator U1, through the DL-1 transfer line, a four-dipole dogleg with an overall R_{56}<1 mm. At the Linac4 exit the beam reaches the 2.4 GeV energy and the DL-2-3 doglegs deliver the beam to the U2-U3 undulators. The lattice from the photoinjector exit up to the DL-1 end has been considered for the modeling of the microbunching instability effect for the SPARX FEL.

Table 1: Electron beam parameter list

Energy	E (GeV)	1.5	2.4
Current	I_{pk} (kA)	1	2.5
Norm. transverse emittance (slice)	ε_{nx} (μrad)	1	1
RMS energy spread (slice)	σ_δ (%)	<0.03	<0.02
Radiation wavelength	λ_r (μm)	13÷3	4÷0.6

Three bunch compressor chicanes are present, BC1, BC2 and BC3, at ≈300-500-1500 MeV respectively. A laser heater chicane is located at the exit of the photoinjector and an X-band cavity for the linearization of the beam longitudinal phase space is foreseen upstream the BC1 magnetic compressor. All the four Linac1-2-3-4 are equipped with three S-band, 3 m long, accelerating sections, with an accelerating gradient of E_{acc}≈23 MV/m. The considered compression schemes are summarized in Table 2.

Table 2: SPARX FEL configurations at Low Energy (LE) and High Energy (HE)

Phase 1-Energy=1.5 GeV	
WP1-LE	RF compression + BC2
WP2-LE	BC1+BC2
Phase 2-Energy= 2.4 GeV	
WP1-HE	RF compression + BC3
WP2-HE	BC1+BC3

THE INPUT BEAM

A 1nC beam, generated by a 10 ps laser pulse profile, has been tracked with the TSTEP code from the photocatode up to the photoinjector exit, becoming the "input beam" for the microbunching instability study along the accelerator. Two cases have been considered: WP1 with factor three RF compression in the first accelerating section, and WP2 with on crest acceleration in the three s-band sections that belong to the SPARC

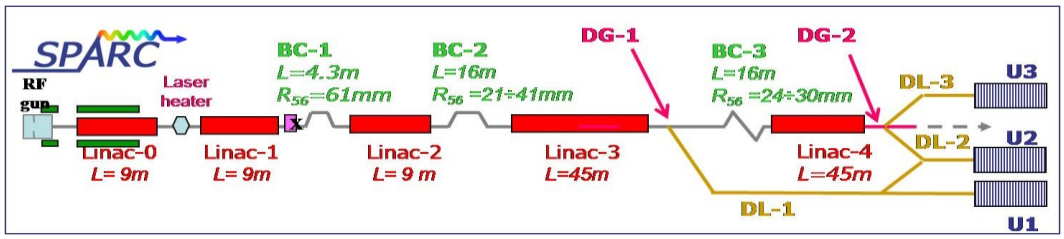

Figure 1: The SPARX Accelerator layout

photoinjector [5]. A density modulation has been applied in both cases at the cathode, with a wavelength λ=150 μm and an amplitude A=10%, simulating a laser pulse fluctuation. Six millions of macroparticles have been used and the resulting two beams are described in Fig. 2 where the rms energy spread and current distributions are reported together with the longitudinal phase space representation, as they are at the exit of the phoinjector.

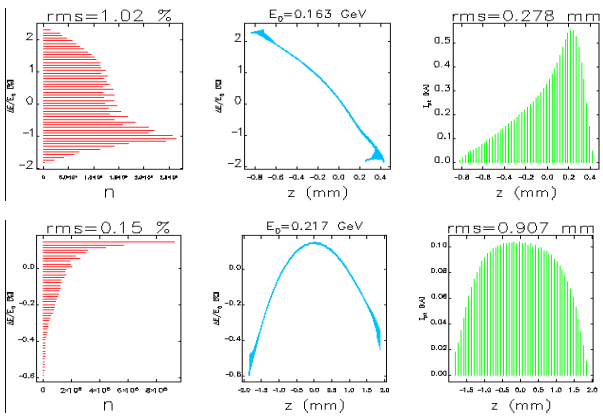

Figure 2: Rms energy spread and current distribution along the bunch, together with the longitudinal phase space for WP1 (above) and WP2 (below) at the photoinjector exit.

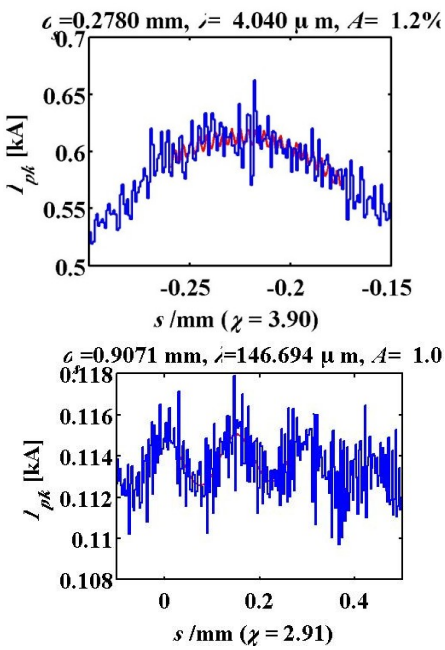

Figure 3: Current longitudinal distribution detail around the maximum value for WP1 (above) and WP2 (below) at the exit of the photoinjector.

From the WP1 longitudinal phase space, Fig. 2 above, it can be seen that applying the RF compression in the photoinjector no longitudinal phase space linearization is required, by means of an X-band section inserted before the following magnetic chicane, as it is instead the case for the WP2 working point where the following bunch compression is purely magnetic, performed by the BC1-BC2 chicanes. Looking in detail around the maximum value of the current distribution along the bunch, Fig.3 above, the "washing out" effect of the initial modulation can be seen due to the applied RF compression at low energy [6], (strong features are still present at the tails of the distribution were the current is low). For the WP2 case the initial modulation is still present at the same wavelength but reduced in amplitude by the space charge effect.

SIMULATION RESULTS

The two input beams for the working points WP1 and WP2 have been tracked with the parallel version of the ELEGANT code [4] from the exit of the photoinjector up to the undulator entrance U1 for the 1.5 GeV case. Scope of the work is to optimize and compare the two compression schemes from the point of view of the microbunching instability effect, laser heater effectiveness, and SASE performance.

The tracking results shown in Fig 4 are obtained switching ON the provided laser heater [7], see Table 3 for parameters, the slice analysis is reported for an applied laser power P=10MW, that it required to lower the resulting slice energy spread around the value of $\sigma_\delta \approx 3\times10^{-4}$.

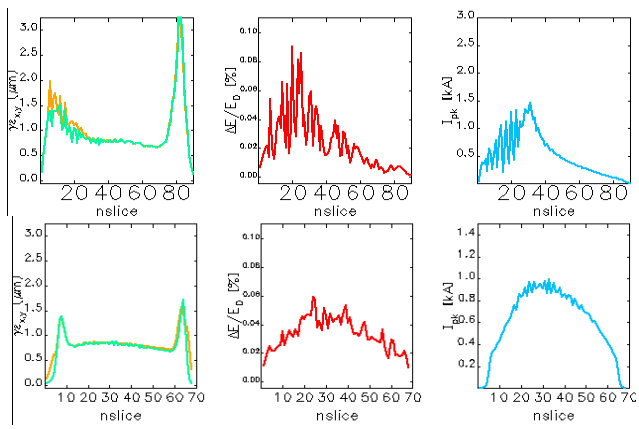

Figure 4: WP1 (above) and WP2 (below) slice emittance, energy spread and current for the 1.5 GeV beam at the DL-1 dogleg exit, as obtained with parallel ELEGANT.

Table 3: Laser Heater parameter list

electron Energy	160 ÷210 MeV
transv. rms beam size	200 μm
undulator period	0.05 m
undulator parameter	3.00÷2.13
undulator length	0.50 m
laser wavelenght	800 nm
laser rms spot size	200 μm

The projected emittance dilution is about 30 % and 10% for WP1 and WP2 respectively. A strong difference can be observed in the resulting slice energy spread as the RF compressed beam seems less sensitive to the laser heater dumping effect; the current slice distribution shows also stronger features in the WP1 case. The analysis has been completed with the Genesis code simulation [8] for the U1 undulator (Table .4). The obtained results have been reported in Fig. 5 where the SASE saturation power vs. the undulator length is shown for the two working points, while in Fig 6 the two radiation spectra are reported.

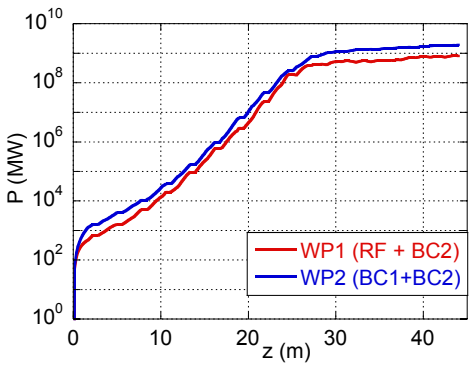

Figure 5: SASE radiation power vs. undulator length as obtained with GENESIS, (λ_r =9 nm)for the two working points WP1-WP2 at 1.5 GeVwith laser heater power P_{LH}=10 MW.

Table 4: U1 (VUV-EV) undulator parameter list

Period	***3.4 cm***
Undulator length	2.278m
No. of Periods	67
Gap (min/max)	8.1 / 25 mm
K max	3.275
Remanent field (effective)	1.2 T
Blocks per period	4

From the point of view of the SASE performance the purely magnetic compression scheme WP2 behave slightly better, even though, despite of the higher slice energy spread, the RF compressed beam shows a slightly higher peak current on the slice, due to its peculiar longitudinal distribution shape, and this helps in reaching the same average saturation length of $L_{sat} \approx 39$ m. This saturation length is well far beyond the U1 undulator length (L_{sat}≈22m) this being intended as a "didactic" case

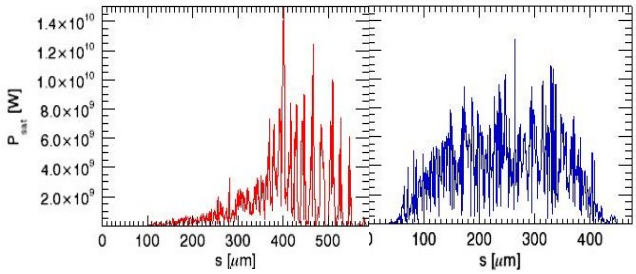

Figure 6: WP1 (red) and WP2 (blue) longitudinal distribution of the saturation power.

where a considerable density modulation has been superimposed to the electron beam at the cathode, just to clarify different aspects of the different beam dynamics for the two working points. It has also to be noticed that one of the main issues associated with the design of a heater device is the amount of power of the laser itself necessary to prevent the growth of the instability. The power should be carefully chosen to avoid over heating, which may be responsible for an energy spread larger than the one to be cured, or sub-heating, if the laser power is not sufficiently intense as pointed in [9], this optimization work is in progress.

CONCLUSIONS

Two different working points WP1 and WP2 have been studied from the point of view of the microbunching instability effect and the laser heater effectiveness in reducing it. The two lattices have been optimized at their best to obtain the beam parameters required for the SASE operation as reported in Table 1. First of all comparing the two lattices it is worth to notice that no X-band longitudinal linearization is needed for the RF compressed beam prior to enter the BC2 magnetic chicane that is instead required for the purely magnetic compression. As far as the output beam is concerned the considered density modulation superimposed at the cathode seems to affect more the hybrid compression scheme (WP1), as it is evident for the final slice energy spread and emittance dilution significantly worse for this case. Nevertheless the SASE performance seems to be not dramatically different for the two cases reasonably due to the higher peak current for the RF compressed beam.

REFERENCES

[1] www.sparx-fel.it, SPARX-TDR-Team.
[2] L. Palumbo *et al*. this conference TUPE022
[3] L.M. Young, priv. comm.
[4] M. Borland," APS- LS-287, September 2000
[5] "The SPARC Project", www.lnf.infn.it/sparc
[6] M. Venturini *et al*., this conference, TUPEC027
[7] Z. Huang, *et al.*, PhysRevSTAB.7.074401
[8] S. Reiche, Nucl. Instr. and Meth. in Phys. Res A, 429 June 1999.
[9] G. Dattoli and M. Migliorati, J. Appl. Phys. 105, 023111 2009